ResearchGate

See discussions, stats, and author profiles for this publication at: https://www.researchgate.net/publication/221883768

Equation of State of a Model Methane Clathrate Cage

ARTICLE *in* THE JOURNAL OF PHYSICAL CHEMISTRY A · MARCH 2012

Impact Factor: 2.69 · DOI: 10.1021/jp2095467 · Source: PubMed

CITATIONS
4

READS
26

3 AUTHORS:

Ruben Santamaria
Universidad Nacional Autónoma de México
41 PUBLICATIONS **390** CITATIONS
SEE PROFILE

Juan Antonio Mondragón Sánchez
Universidad Iberoamericana Puebla
10 PUBLICATIONS **44** CITATIONS
SEE PROFILE

Xim Bokhimi
Universidad Nacional Autónoma de México
115 PUBLICATIONS **2,476** CITATIONS
SEE PROFILE

Available from: Ruben Santamaria
Retrieved on: 26 January 2016

THE JOURNAL OF PHYSICAL CHEMISTRY A

Article

pubs.acs.org/JPCA

Equation of State of a Model Methane Clathrate Cage

Ruben Santamaria,*[,†] Juan Antonio Mondragón-Sánchez,[†,‡,#] and Xim Bokhimi[†,#]

[†]Instituto de Física, Universidad Nacional Autónoma de México, A.P. 20-364, D.F. México

[‡]Instituto de Fisica, Benemérita Universidad Autónoma de Puebla, C.P. 72570, Puebla, México

ABSTRACT: We investigate the behavior of a model methane clathrate cage under high hydrostatic pressures. The methane clathrate cage consists of 20 water molecules forming 12 pentagonal faces, with a methane molecule positioned at the cage center. The clathrate compound is located inside a fullerene-type arrangement of 180 He atoms to simulate an isotropic pressure. Different pressures are simulated by decreasing the radius of the He array. The minimal energy of the total system for each configuration is calculated by using density functional theory. The variation of the energy with the volume of the imprisoned clathrate cage leads to the proposal of a (cold) equation of state in the pressure range [0,60] GPa. The elastic parameters of the state equation are found in agreement with equivalent quantities measured on clathrates in their *sI* conformation. Special attention is given to the distribution of the confined atoms and the eventual symmetry lost from the clathrate cage with the pressure, as the clathrate cage constitutes a basic structural unit of the crystal. Finally, the strengths and limitations of the model are discussed.

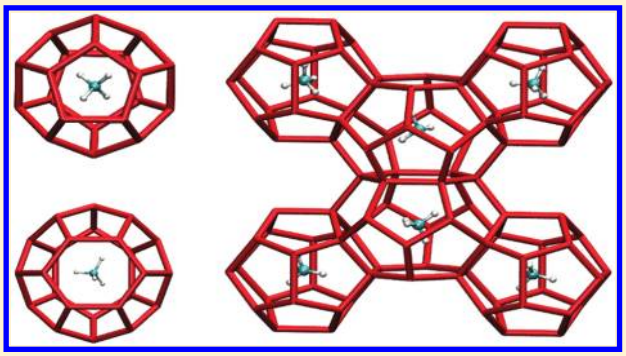

INTRODUCTION

Gas hydrates are structures of water which form periodic interconnected cages and contain small gas molecules in their interiors.[1] When the confined gas compounds are methane molecules (CH_4), the ice-like crystal structure is referred to as *methane clathrate* or *methane hydrate*. This type of hydrate is of particular interest, as great quantities have been found under the sea floor. In fact, a total amount of 30% of the planet's methane is estimated to be in the form of methane clathrate.[2] The methane hydrates are also observed in astronomical objects such as the cool nebula, believed to participate in the formation of planets and their moons. When the nebula is under strong gravitational contraction, the gas hydrates are squeezed, releasing methane, which eventually constitutes one of the main components of the planet's atmosphere. The largest moon of Saturn, Titan, is an example of this process.[3,4] From a technological point of view, methane hydrates have received attention from industries and nation governments because it is a fuel; in other words, methane hydrates are capable to deliver energy. The extraordinary sources of methane hydrates found in our planet make this compound unique and an alternative proposal to solve the energy crisis.[5]

The gas hydrates adopt different conformations depending on the structure of the enclosed guest molecule and the experimental conditions of formation.[1] Three typical crystalline structures have been identified at low pressure (less than 0.5 MPa): the cubic *sI*, the cubic *sII*, and the hexagonal *sH*. The majority of the gas hydrates present *sI* or *sII* structures, as in the case of methane hydrates.[6] On the contrary, only a few gas hydrates with *sH* conformation are observed at low pressures. At pressures greater than 0.5 GPa, the gas hydrates may also adopt an *sH* structure, or a tetragonal structure *sT*, or the *sO* structure, which is closely related to the ice structure *Ih* (refer to refs 2 and 7 for a review). The gas hydrates at *low pressures* have been studied extensively in recent decades;[1,2,7] nevertheless, research on these systems at *high pressures* is recent.[2,7] The most common experimental techniques used in the high pressure regime are Raman spectroscopy,[8−11] X-ray crystallography,[8,12−15] and neutron diffraction.[13,14] Two phase transitions have been observed for methane hydrates in the high pressure range: $sI \rightarrow sH \rightarrow sO$, with a possible intermediary conversion from $sI \rightarrow sII$ before reaching the *sH* conformation. The evidence indicates that results strongly depend on the experimental conditions.

With respect to theoretical studies on methane hydrates, these have been mainly based on molecular dynamics simulations. Many of them are devoted, for instance, to the investigation of thermophysical aspects,[16] such as formation and growth[17−20] and structural stability.[21,22] Other works have focused attention on the dynamics of molecules,[23,24] dissociation and decomposition of the structure,[25−28] thermal conduction,[29,30] inhibition of structural formation,[31−33] crystallite nucleation,[19,34−36] etc.

The goal of the present work is to analyze the pressure-modulated behavior of a model methane clathrate cage. The investigation has resort to the thermodynamic model of finite size systems (TMoFSS) described elsewhere.[37,40] Still, it is briefly discussed here for completeness (though other approaches to nanothermodynamics exist[41]). We perform a hydrostatic-pressure

Received: October 3, 2011
Revised: March 2, 2012
Published: March 2, 2012

ACS Publications © 2012 American Chemical Society

process on the model methane clathrate cage, without the consideration of temperature effects. It is from the variation of the energy with the volume that we are able to formulate a "cold" *PV* equation of state. The methane clathrate cage constitutes one of the basic structural units of the crystal, and the results should complement the characterization of the crystal phase diagram. The investigation is important, as methane clathrates are considered a new class of energy source with potential use in the immediate future (refer to the U.S. DOE report).[42] The work is structured as follows: the compression model and electronic structure method are briefly discussed in the next two sections. The results concerning the structures of methane clathrate under different pressures are given in a subsequent section. The state equation is formulated in this part of the body text. The results are compared with experimental observations whenever possible. The main conclusions appear in the last section, focusing on the behavior of the methane clathrate cage under high pressure.

CONFINEMENT MODEL

Endohedral Confinement. Methane hydrate crystallizes in the cubic structure *sI*, whose unit cell is conformed by two 5^{12} and six $5^{12}6^2$ water cavities. The nomenclature 5^{12} indicates a cage with 12 pentagonal faces made out of 20 water molecules (Figure 1A) and $5^{12}6^2$ is a cage with 12 pentagonal faces plus 2 hexagonal faces formed with 24 water molecules (Figure 1B). The structure of the *sI* crystal including the unit cell (Figure 1C) is depicted in Figure 1.

The $5^{12}6^2$ cages have been studied more abundantly in molecular dynamics simulations[32] than their 5^{12} counterparts. In this work we chose the less common 5^{12} structure as the model methane clathrate cage. In order to simulate pressure effects on the methane clathrate cage, the cage was located inside a fullerene-type structure He_{180}. The structure was constructed with He inert atoms to minimize chemical reactions with the clathrate. The confining structure is essentially spherical and, for that reason, we refer to it as the confining sphere. The confining sphere was maintained rigid during the calculations. The pressure effects were produced by changing the radius of the sphere. The compression is isotropic due to the spherical shape of the confining structure. Strictly speaking, the compression of a single cage cannot be considered the counterpart of compression of the real clathrate hydrate crystal in experiments. Still, the cage is one of the main structural components of the clathrate crystal and, consequently, represents an important contribution to the elasticity of the crystal due to the flexibility of the cages. More drastic approximations have suggested that the Young moduli computed between pairs of atoms constitutes a good first descriptor of the crystal elasticity. Clearly, the model presented here goes beyond such a simplification. There is an additional point to discuss: the real clathrate structure shows no dangling bonds, while in the model we have dangling bonds (this is the cost for dealing with a finite size system). Still, the energetic impact of dangling bonds in the "energy versus volume" curve (to be computed later) is considered to be small. It is due to the fact that, in going from one oxygen atom to a neighboring oxygen atom, the hydrogen dangling bonds take a minimum energy, as the energy barriers are small. On the other hand, excessive pressure is expected to destroy the clathrate cage structure and, in this connection is consistent with the results expected at high pressures. Certainly, a way to improve upon the present model is to include more structure of the clathrate crystal. The model and analysis follow lines analogous to those of confined hydrogen clusters.[37−40] The confining sphere, with a methane hydrate cage in the interior, is illustrated in Figure 2.

In a first stage, the methane clathrate cage structure was energetically optimized in vacuum. Later, it was inserted in the He spherical cage. By maintaining the rigidity of the spherical cage, the methane hydrate was allowed to relax, thus achieving a minimal energy. The relaxation permits observation of local disorder, as, for instance, the hydrogen atoms may assume different orientations due to the pressure exerted by nonequivalent (pentagons and hexagons) atoms of the fullerene sphere. In a second stage, the radius of the spherical cage, with the methane hydrate in the interior, was slightly reduced to produce a higher pressure. The last step was repeated several times.

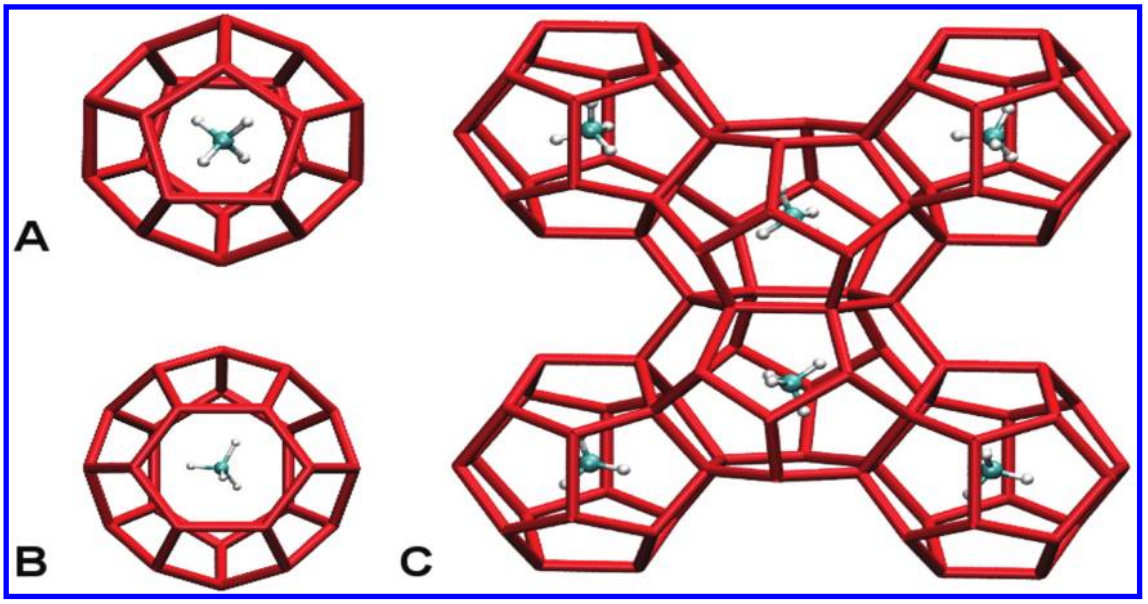

Figure 1. Representation of both the 5^{12} and $5^{12}6^2$ water cages (panels A and B, respectively) and part of the methane hydrate unit cell of the *sI* crystal structure (panel C). The crystal structure was built from ref 43. The basic components of the *sI* crystal are the 5^{12} and $5^{12}6^2$ water cages. The guest molecules are methane compounds. Clathrate hydrogens are omitted for simplicity.

dx.doi.org/10.1021/jp2095467 | J. Phys. Chem. A 2012, 116, 3673−3680

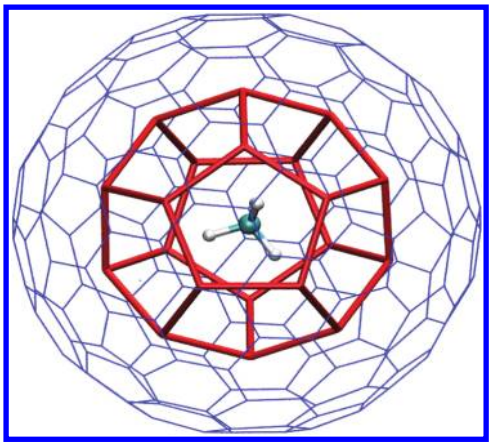

Figure 2. A fullerene-like sphere of 180 He atoms is used to compress the 5^{12} clathrate unit with a methane inside the clathrate.

In this sequence of events, the optimized clathrate molecule was used as the initial entry of the next optimization. The calculation process simulates a hydrostatic pressure. We refer to the pressure as a *cold pressure* because no vibrations nor thermal motions of the confined particles were considered. The finite size of the model permits analysis of local properties solely, as it does not take long-range effects into account, such as lattice vibrations. According to observations on the laboratory synthesis, different phases of clathrate cages are produced by controlling the temperature, pressure, and compression time rate. In our model, the temperature and compression time rate are not considered because we are interested in exclusively evaluating pressure effects (though temperature effects and time rates may be considered following the instructions in ref 44).

Pressure. The following formulation is of general validity for systems containing a small or large number of particles. It has been discussed in detail elsewhere,[37,40] but it is briefly discussed next. We require determination of the energy E and volume V of the confined particles to establish the equation of state because the static pressure P is given in terms of such basic variables.

$$P = -(\partial E/\partial V)_{N,T} \tag{1}$$

The dynamic or thermal pressure at low temperatures contributes little to the total pressure (though it may be important to induce a phase transition). In this regard, the cold pressure is the most representative term in the equation of state at low temperature conditions. The total energy E_{tot} of the system, conformed by atoms of the confining sphere plus the pressurized methane clathrate atoms, is computed for every radius of the confining sphere. The energy E of eq 1 is obtained by subtracting the energy of the confining sphere E_{sph} from the total energy E_{tot}.

$$E(\overline{R}_{sph}) = E_{tot}(\overline{R}_{sph}) - E_{sph}(\overline{R}_{sph}) \tag{2}$$

The radius of the confining sphere $\overline{R}_{sph}$ is maintained constant in the calculation of the energies (bars over variables signify average values).

Volume. The volume of the confined particles is required to determine the pressure. The volume of the confined clathrate particles is obtained from the average sphere radius $\overline{R}_{sph}$:

$$\overline{R}_{sph} = \sum_{i=1}^{M} R_i/M \tag{3}$$

where R_i is the distance of the ith sphere atom to the sphere center and M is the number of sphere atoms. The effective radius R_p of the confined particles is:

$$R_p = \frac{1}{3}(\overline{R}_O + \delta R_O) + \frac{2}{3}(\overline{R}_H + \delta R_H) \tag{4}$$

The quantity $\overline{R}_O$ is the average distance of the enclosed oxygen atoms to the sphere center and $\overline{R}_H$ of the enclosed hydrogen atoms to the sphere center. The coefficients 2/3 and 1/3 are weight factors associated to the number of hydrogen atoms relative to the oxygen atoms. The electron cloud of the imprisoned atoms also takes a volume, not considered in the terms $\overline{R}_O$ and $\overline{R}_H$. The electron cloud of the enclosed atoms forms a shell around them (Figure 3). This electron shell is considered

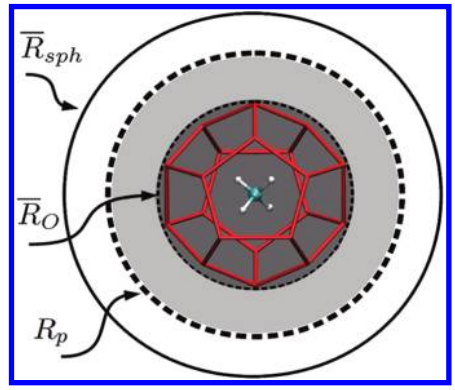

Figure 3. The electron cloud of the confined particles takes a volume (illustrated with both shadow areas) and appears delimited with strong dashed lines in the Figure. Such a volume is considered in the computation of the pressure (eq 1). The quantity $\overline{R}_{sph}$ is the radius (eq 3) of the confining sphere, R_p the effective radius (eq 4) of the imprisoned molecule, and $\overline{R}_O$ the radius of the clathrate oxygen atoms (illustrated with darker area and delimited by soft dashed lines). Hydrogens are omitted for clarity.

through the correction terms δR_O and δR_H for oxygens and hydrogens, respectively. The electron contributions δR_O and δR_H are computed from $\overline{R}_{sph}$, $\overline{R}_O$, and $\overline{R}_H$, and from the new quantities R_O^{corr} and R_H^{corr}

$$\delta R_O = (\overline{R}_{sph} - \overline{R}_O)(1 - R_O^{corr})/2$$
$$\delta R_H = (\overline{R}_{sph} - \overline{R}_H)(1 - R_H^{corr})/2 \tag{5}$$

The terms $\overline{R}_{sph}$, $\overline{R}_O$, and $\overline{R}_H$ were defined above; therefore, the discussion of the corrections R_O^{corr} and R_H^{corr} for oxygen and hydrogen now follows. These corrections depend on the nature of both the sphere atoms and confined atoms. They are given in the form:

$$R_O^{corr} = u_O/(u_O{}^2 - 1) \qquad u_O = (\chi_O - 1)/(\chi_O + 1) \qquad \chi_O = R_O/R_{He}$$
$$R_H^{corr} = u_H/(u_H{}^2 - 1) \qquad u_H = (\chi_H - 1)/(\chi_H + 1) \qquad \chi_H = R_H/R_{He} \tag{6}$$

where the radii $R_O = 0.4652$, $R_H = 0.5292$, and $R_{He} = 0.3113$ correspond, in that order, to the Bragg–Slater radius of oxygen,

dx.doi.org/10.1021/jp2095467 | J. Phys. Chem. A 2012, 116, 3673–3680

hydrogen, and helium.[45] The ionic radius of helium is more compact than that of hydrogen and oxygen and, in turn, the ionic radius of oxygen is smaller than that of hydrogen. The contributions R_O^{corr} and R_H^{corr} follow Becke's proposal for the decomposition of molecular functions into single-center components.[46] In our case, the correction terms R_O^{corr} and R_H^{corr} that appear in eqs 5 have negative signs, thus increasing the effective radii of the oxygen and hydrogen atoms obtained with the contributions $\bar{R}_O + (\bar{R}_{sph} - \bar{R}_O)/2$ and $\bar{R}_H + (\bar{R}_{sph} - \bar{R}_H)/2$ solely. When the sphere atoms and enclosed atoms are of the same species, the space between them is equally shared by their electron clouds. In this particular case, we have $\chi_O = 1$ and $\chi_H = 1$ and, therefore, $R_O^{corr} = 0$ and $R_H^{corr} = 0$. In other words, the contribution of the electron cloud to the confining radius corresponds to half the distance between the sphere atoms and enclosed atoms. On the other hand, when the volume of the confined particles is large enough, the corrections δR_O and δR_H are very small and can be neglected. This case occurs when dealing with, for example, a large number of confined particles. The corrections proposed in eqs 4−6 generalize the method presented in refs 39 and 40.

Finally, because the atoms under confinment are energetically optimized (see section below) and, in addition, the pressure is equally exerted over each confined atom, the sphere is considered to be uniformly filled or homogeneously pressurized in the interior. In this case, the volume of the pressurized particles corresponds to that of a uniform sphere with confining radius R_p (eq 4).

$$V_p = (4\pi/3)R_p^3 \tag{7}$$

As an example of the calculation of the effective radius R_p of the confined particles, let us consider an average sphere radius of $\bar{R}_{sph} = 7.900$ Å. For this value, the average distance of the enclosed oxygen (hydrogen) atoms in the optimized clathrate structure is $\bar{R}_O = 3.694$ Å ($\bar{R}_H = 3.813$ Å). By using $\bar{R}_{sph} = 7.900$ Å in eq 5, we obtain $\delta R_O = 2.537$ Å ($\delta R_H = 2.612$ Å), where we have previously computed $R_O^{corr} = -0.206$ ($R_H^{corr} = -0.278$) from eq 6. We obtain $R_p = 6.360$ Å when the values are introduced in eq 4.

METHOD

We use density functional theory (DFT) for the computation of energies. In this approximation, the electron wave function is represented by a single determinant of molecular orbitals, which in turn are determined by self-consistently solving the DFT Kohn−Sham one-electron equations. Basis sets of the type 6-31g produce small basis set superposition errors and are used to build the molecular orbitals. Fine grids are used in the numerical integrations with tight convergence criteria. The integration scheme ensures an energy accuracy of 10^{-7} au. We use the generalized-gradient version of DFT with the expressions of Becke for exchange[47] and Lee−Yang−Parr for correlation.[48] In principle, they are appropriate for investigating energetic features of systems with highly inhomogeneous charge distributions.

We neglected the zero-point vibration energy contribution of the guest molecule to the pressure in the calculations. It was mainly due to the following reasons: (i) the zero-point vibration of the confined guest molecule was observed in ref 37 to be essentially constant and small in a relatively large pressure range (up to a few hundreds of GPa), and (ii) we dealt with relative energies, where the reference energy was this of the highest compressed structure, thus producing to some extent the cancelation of vibrational energies. In this context, zero-point energy contributions of the guest molecule (CH_4) were neglected, without significant loss of accuracy in the equation of state.

The energy-optimized structures of the encapsulated atoms were obtained with resort to the subroutine of Kaestner (optimization algorithm L-BFGS[49]), and using dynamic DFT grids, switching from single to double precision arithmetics in the energy convergence process. Thresholds in the energy (1.0×10^{-6} hartree), maximum step (1.8×10^{-3} bohr), rms step (1.2×10^{-3} bohr), maximum gradient (4.5×10^{-4}/bohr), and rms gradient (3.0×10^{-4}/bohr) were imposed. The confinement model and method are fully compatible with the new graphical process unit (GPU) supercomputing technologies and strategies discussed in ref 50. The calculations are performed on a Fermi cluster with four GPUs, making use of the *TeraChem* Cuda-code program.[51,52]

RESULTS AND DISCUSSION

A sequence of calculations were performed for a sphere radius $\bar{R}_{sph}$ with values from 7.90 down to 4.77 Å. In terms of the R_p confining radius, the interval goes from 6.36 down to 4.08 Å (in other words, from low to high pressures). The energy E (eq 2) in terms of the confining volume V_p (eq 7) is plotted in Figure 4 (solid blue circles). The energy exhibits an exponential profile due to the general repulsive character of the potential energy when the particles get close together.

The pressure is obtained from eq 1, by differentiation of the energy with respect to the confining volume. However, in order to carry a numerical derivative from numerical data, we require energy points sufficiently close to each other to have a smooth and well behaved pressure. In our case, the energy points are not really sufficiently close. This is the main reason we must parametrize the numerical data. Two parametric curves of the numerical data are also depicted in Figure 4: the one in red is due to Vinet and collaborators[53] and the one in green to Liu and collaborators.[54] The parametric curve of Vinet is:

$$E_{Vin} = -\frac{9B_0V_0}{\eta^2}[1 - \eta(1 - x)]\exp[\eta(1 - x)]$$
$$x = (V_p/V_0)^{1/3} \qquad \eta = \frac{3}{2}(B_0' - 1) \tag{8}$$

The parameters B_0, B'_0 and V_0 are obtained by fitting the Vinet's curve to the numerical data. In this regard, no analytical expressions are required for them. However, according to Vinet, they are interpreted as the isothermal bulk modulus and its first pressure derivative at zero pressure, while V_0 is usually considered the zero-pressure volume. It is important to remark that the Vinet's equation of state is considered a universal expression, it was deduced after experimental investigation on the energetics and isothermal behavior of compressed systems, and has been additionally validated for a number of solids under compression. In the absence of phase transitions, the Vinet's expression was created from knowledge of the zero-volume pressure, the isothermal compression and its first derivative. In short, the state equation of Vinet is applicable to our system of particles under compression, together with the original

dx.doi.org/10.1021/jp2095467 | J. Phys. Chem. A 2012, 116, 3673−3680

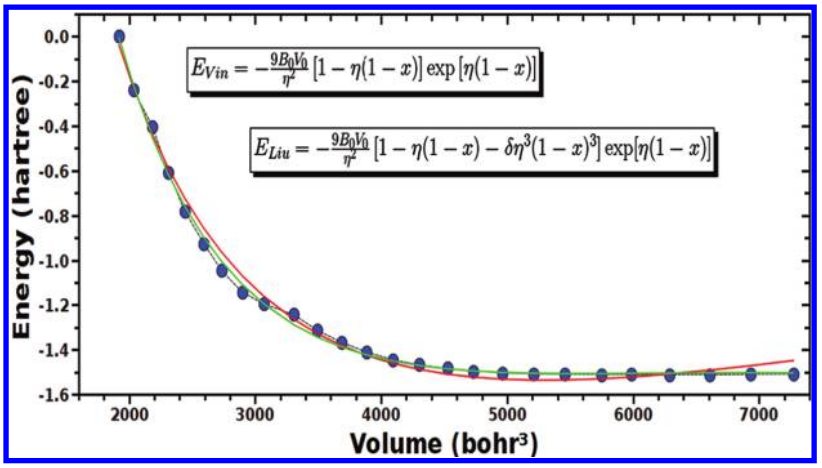

Figure 4. The energy E (eq 2) of the imprisoned methane clathrate in terms of the confining volume V_p (eq 7) is depicted (solid blue circles). Two parametrizations of E vs V_p using the expressions of Vinet (red line, eq 8) and Liu (green line, eq 9) are also sketched.

interpretation of its parameters. On the other hand, the parametric curve of Liu is:

$$E_{\mathrm{Liu}} = -\frac{9B_0V_0}{\eta^2}[1 - \eta(1-x) - \delta\eta^3(1-x)^3] \times \exp[\eta(1-x)]$$
$$\eta = \sqrt{\frac{9B_0V_0}{E_c}} \qquad \delta = \frac{B_0' - 1}{2\eta} - \frac{1}{3} \tag{9}$$

The basic parameters are B_0, B'_0, V_0, and E_c, and the dependent parameters are η and δ. The B'_0, η, and δ parameters are dimensionless, while B_0 and V_0 have units of hartree/bohr^3 (pressure) and bohr^3 (volume), respectively. The Liu expression contains an additional parameter (δ) with respect to the Vinet expression, and reproduces the Vinet equation when $\delta = 0$ as, in this case, $\eta = (3/2)(B'_0 - 1)$ and the expression containing E_c is simply neglected, to have $E_{\mathrm{Vin}} = E_{\mathrm{Liu}}$. The parameters exhibit a complex landscape where different sets of parameters are observed to reproduce the numerical data. However, not all the sets are acceptable from a physical perspective, as negative values of B_0 and V_0 must be avoided. The set of parameters reproducing the numerical data and satisfying the physical constraints are given in Table 1.

Table 1. Parameter Values of the State Equations of Vinet (eq 8) and Liu (eq 9)[a]

parameter	Vinet	Liu
B_0	3.8311×10^{-4}	1.0378×10^{-4}
B'_0	3.2990	11.7221
V_0	5299.9334	5584.6479
η	3.4485	1.8600
E_c		1.5077
δ		2.5490

[a]The independent and dependent parameters of Vinet and Liu are included for comparison. The parameters B'_0, η, and δ are dimensionless and B_0 and V_0 have units of hartree/bohr^3 (pressure) and bohr^3 (volume), respectively.

The parameters B_0, B'_0, and V_0 of Vinet and Liu exhibit noticeable differences. The δ factor of Liu is 2.55, distant from zero, indicating large differences between the Liu and Vinet equations of state. Still, we use both parametrizations to compute the pressure, with careful interpretation of the elastic mechanical parameters that appear in the Liu and Vinet expressions. According to eq 1, the pressure is obtained by straightforward differentiation of the energy. In this regard, the Vinet and Liu expressions of the pressure are:

$$P_{\mathrm{Vin}} = \frac{3B_0(1-x)}{x^2}\exp[\eta(1-x)]$$
$$P_{\mathrm{Liu}} = \frac{3B_0(1-x)}{x^2}[1 + 3\delta\eta(1-x) + \delta\eta^2(1-x)^2] \times \exp[\eta(1-x)] \tag{10}$$

Figure 5 shows the two state equations using the parameters of Table 1. The pressure essentially runs from a few GPa to 60 GPa. There are several equations of state proposed for solids of different nature such as, for example, the Rose equation;[55] nevertheless, the Vinet equation is considered to be universal for several categories of solids and, for this reason, it has been extensively studied.[56] Despite that, the Vinet equation has shown to present slight deviations of the isothermal bulk modulus.[57] The experimental values of H_2O−ice VII referent to the isothermal bulk modulus and its first pressure derivative at room temperature are, respectively, B_0 = 23.9 GPa and B'_0 = 4.2, while the zero-pressure volume is V_0 = 12.3 cm^3/mol.[58] On the other hand, the estimated isothermal Young moduli of the *sI* and *sII* hydrates at 268 K are, in that order, 8.4 and 8.2 GPa.[1] The mechanical elastic parameters of ice−water differ from those of *sI* and *sII* hydrates due to the different conformations adopted by water molecules. Thereby, care should be taken when comparing against the mechanical properties of ice−water. In our case, the Vinet parameters are B_0 = 11.3 GPa and B'_0 = 3.30, while the Liu parameters are B_0 = 3.05 GPa and B'_0 = 11.7. If we assume that the clathrates classify in the category of compounds where the Poisson's ratio is approximately 0.33, then the Young moduli given above (8.4 and 8.2 GPa) are equivalent to the bulk moduli.[59] In this regard, the Vinet parameters are closer to the experimental values than the Liu parameters. However, it is important to remark that the state equation applies to the clathrate cage, while the experimental values are due to the crystal structure. Therefore, the precise reproduction of the crystal values should not be formally expected.

dx.doi.org/10.1021/jp2095467 | J. Phys. Chem. A 2012, 116, 3673−3680

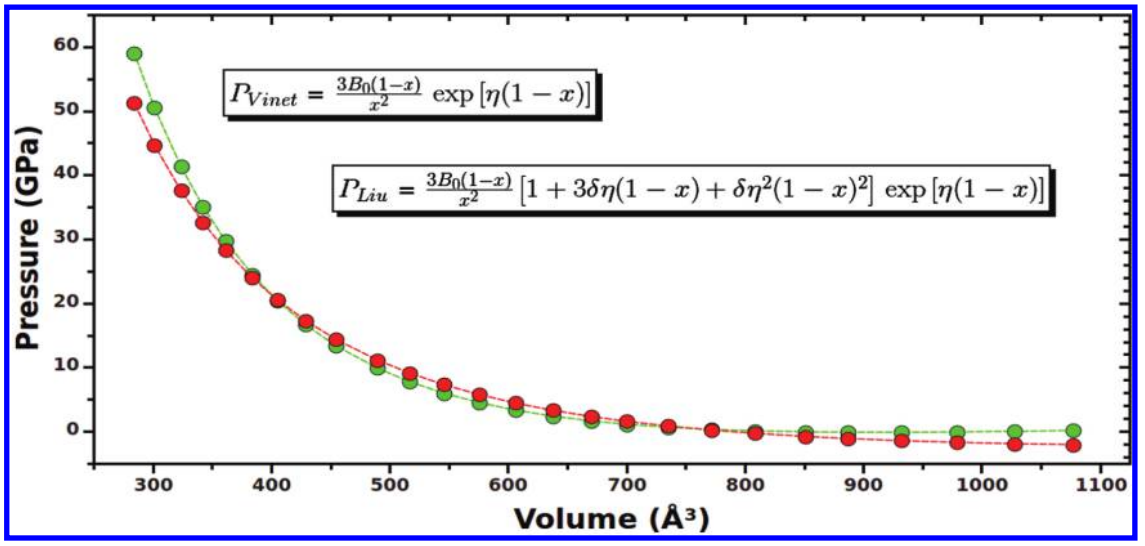

Figure 5. The Vinet and Liu expressions of the pressure (eqs 10) are plotted against the volume (eq 7). The Vinet line appears in red color and the Liu line in green color.

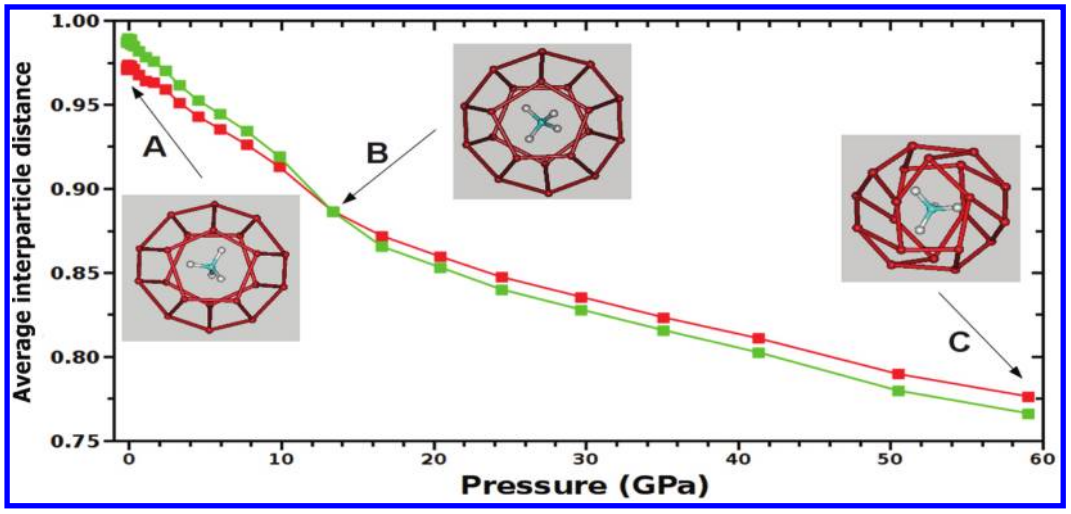

Figure 6. The average (dimensionless) interparticle distances (eq 11) in terms of the pressure are plotted. The expression of Liu (eq 10) was used to compute the pressure. The interparticle distances of the oxygens appear in red color and those of hydrogens in green color. The insets show the pressure-induced structures of the methane clathrate cage (similar orientations are given for comparison, and hydrogens are omitted for clarity). At intermediate pressures (~13 GPa), the hydrogen atoms originally bonded to their oxygens change bonds with contiguous oxygen atoms. At high pressures (~60 GPa), the methane clathrate cage has lost the characteristic structural symmetry observed at low pressures (at less than 5 GPa).

In our model, a sphere of radius of $\overline{R}_{sph}$ = 7.90 Å (P_{Liu} = 0.1 GPa) corresponds to a density of 0.56 g/cm^3, and for a sphere radius of $\overline{R}_{sph}$ = 6.08 Å (P_{Liu} = 4.5 GPa), the density has approximately increased 2-fold, more precisely, 1.05 g/cm^3. Thus, the mass density is sensitive to the pressure and, apparently, to the temperature as well (the density of methane clathrate is 0.91 at 273 K and 0.94 g/cm^3 at 277 K in the *sI* and *sII* conformations, respectively, see ref 60 for calculation details).

The guest molecule is important in the stability of the clathrate by imparting, with its presence, rigidity to clathrate cage. Still, structural changes of the clathrate cage are induced by the hydrostatic pressure. At low pressures, the structural changes start with the migration of hydrogen atoms of some oxygens to contiguous oxygens; nevertheless, the oxygen atoms (the heavier elements in this case) show small positional displacements compared with the light atoms (inset A of Figure 6). In the intermediate pressure range, some hydrogens start to migrate to the interior part of the clathrate cage (inset B of Figure 6 with pressure ~13 GPa). Finally, in the high pressure range, the clathrate cage loses its characteristic structural symmetry and can not be classified in terms of symmetry elements anymore (inset C of Figure 6 with pressure ~60 GPa).

In order to measure the packing degree of the clathrate cage, we have recourse to the average (dimensionless) internuclear distance d defined in the form:

$$d = \sum_{j>i} d_{i,j}/d_0 \qquad (11)$$

where d_{ij} is the distance between atoms i and j, and d_0 is the normalization factor that corresponds to the sum of internuclear distances of the clathrate cage in vacuum. The distance d is independent of the origin. The main purpose of d is not to describe details of the cage structure but rather to quantify with a single number the average shrinking of the cage with the pressure. In this regard, it is straightforward to compare the behavior of oxygens and hydrogens under compression by

dx.doi.org/10.1021/jp2095467 | J. Phys. Chem. A 2012, 116, 3673–3680

making use of the d parameter. The subindexes in eq 11 run over the total number of atoms: the total number of distances for oxygens is $20 \times 19/2 = 190$ and for hydrogens is $40 \times 39/2 = 780$. A value of d different from 1 points out a structural change of the clathrate cage with respect to the value in vacuum: when it is lower than 1, there is a contraction of the cage, and when the value is larger than 1, there is an expansion. At small pressures, the value of d decreases but the symmetry of the clathrate cage is preserved. A cross point of the oxygen and hydrogen curves occurs at a pressure of 13 GPa. It is due to the breaking of some hydrogen bonds. In this case, the hydrogens migrate toward the inner part of the cage. The new locations of these hydrogens reduce the value of d. At high pressures, more evident changes occur; for instance, at 60 GPa, the clathrate cage has approximately shrunk one-fourth of its original value with total loss of the symmetry. Because the clathrate cage conforms to a basic structural unit of the crystal, we also expect it to conform to an *elastic mechanical unit*, which to a great extent contributes to the elastic parameters of clathrate hydrates of natural gases, thus complementing the characterization of the phase diagram. On the other hand, note that experimental studies based on Raman spectroscopy of gas hydrates at high pressure indicate that methane hydrates initially in the *sI* conformation get transformed to the *sH* conformation around 1 GPa, subsequently transforming from the *sH* to the *sO* conformation around ~2 GPa. Whereas *sI* and *sH* contain 5^{12} polyhedra (and others types as well), the *sO* conformation shows no water polyhedra and forms a structure closely related to ice *Ih*. The model illustrated in this work is not expected to show such transitions, as we have only restricted our study to a basic unit of the clathrate crystal. Despite that, the model remains valid for larger and representative structures of the clathrate crystal. Work in this direction is in progress.

CONCLUSIONS

Methane clathrates are structures of scientific and technological interest due to their interplanetary roles and energy implications. We have presented a model of confinement that explicitly exhibits atomic structure to mimic pressure on either small or large molecules. The model makes use of a fullerene-type sphere formed by inert helium atoms enclosing a small 5^{12} polyhedron structure of the methane clathrate crystal. The total number of atoms in this particular case was 245. Several isotropic pressures were generated by reducing the sphere radius, without taking temperature effects into consideration. The energy in terms of the clathrate cage volume was plotted and parametrized based on the expressions of Vinet and Liu. The process led to the proposal of a cold equation of state. Despite dealing with just one of the basic units of the clathrate crystal, the elastic parameters of the state equation were found to be close to the experimental ones. Structural deformations of the methane clathrate cage with the pressure were analyzed in the [0,60] GPa and discussed. A progressive deformation of the methane clathrate cage is observed with the pressure. The hydrogens are the first entities to migrate at relatively low pressures. At the intermediate pressure range, the hydrogens start to occupy positions inside the clathrate cage. At high pressures, the clathrate cage symmetry is lost. The confinement model is easily generalizable, for instance, by using confining cages with geometries different from the spherical one, thus producing anisotropic pressures, or by changing the atomic structure of the confining sphere, etc. The confinement model is fully compatible with GPU technology because all the calculations can be performed in GPUs, such as for a big molecule, with little resort to CPUs.

AUTHOR INFORMATION

Corresponding Author

*E-mail: rso@fisica.unam.mx (R.S.).

Additional Author Information

[#]E-mail: jantonioms@gmail.com (J.A.M.S.)

[#]E-mail: bokhimi@fisica.unam.mx (X.B.).

Notes

The authors declare no competing financial interest.

ACKNOWLEDGMENTS

J.A.M.S. acknowledges LAREC-IFUNAM for financial support.

REFERENCES

(1) Sloan, E. D.; Koh, C. A. *Clathrate hydrates of natural gases*; CRC Press: New York, 2007.

(2) Loveday, J. S.; Nelmes, R. J. *Phys. Chem. Chem. Phys.* **2008**, *10*, 937−950.

(3) Lunine, J. I.; Stevenson, D. J. *Icarus* **1987**, *70*, 61−77.

(4) Atreya, S. K.; Lorenz, R. D.; Waite, J. H. Volatile origin and cycles: nitrogen and methane. In *Titan from Cassini-Huygens*; Brown, R. H., Lebreton, J. P., Waite, J. H., Eds.; Springer Dorderscht: Heidelberg, 2010; Chap. 7, pp 177−199.

(5) Demirbas, A. *Methane gas hydrate*; Springer-Verlag: London, 2010.

(6) Sloan, E. D. *Nature* **2003**, *426*, 353−363.

(7) Fortes, A. D.; Choukroun, M. *Space Sci. Rev.* **2010**, *153*, 185−218.

(8) Hirai, H.; Uchihara, Y.; Fujihisa, H.; Sakashita, M.; Katoh, E.; Aoki, K.; Nagashima, K.; Yamamoto, Y.; Yagi, T. *J. Chem. Phys.* **2001**, *115*, 7066−7070.

(9) Shimizu, H.; Kumazaki, T.; Kume, T.; Sasaki, S. *J. Phys. Chem. B* **2002**, *106*, 30−33.

(10) Choukroun, M.; Morizet, Y.; Grasset, O. *J. Raman Spectrosc.* **2007**, *38*, 440−451.

(11) Ohtani, T.; Ohno, Y.; Sasaki, S.; Kume, T.; Shimizu, H. *J. Phys: Conf. Ser.* **2010**, *215*, 012058.

(12) Machida, S. I.; Hirai, H.; Kawamura, T.; Yamamoto, Y.; Yagi, T. *Phys. Earth Planet.* **2006**, *155*, 170−176.

(13) Loveday, J. S.; Nelmes, R. J.; Guthrie, M.; Klug, D. D.; Tse, J. S. *Phys. Rev. Lett.* **2001**, *87*, 215501.

(14) Loveday, J. S.; Nelmes, R. J.; Klug, D. D.; Tse, J. S.; Desgreniers, S. *Can. J. Phys.* **2003**, *81*, 539−544.

(15) Hiraia, H.; Tanaka, T.; Kawamura, T.; Yamamoto, Y.; Yagi, Y. *J. Phys. Chem. Solids* **2004**, *65*, 1555−1559.

(16) Chialvo, A. A.; Houssa, M.; Cummings, P. T. *J. Phys. Chem. B* **2002**, *106*, 442−451.

(17) Moon, C.; Taylor, P. C.; Rodger, P. M. *J. Am. Chem. Soc.* **2003**, *125*, 4706−4707.

(18) Zhang, J.; Hawtin, R. W.; Yang, Y.; Nakagava, E.; Rivero, M.; Choi, S. K.; Rodger, P. M. *J. Phys. Chem. B* **2008**, *112*, 10608−10618.

(19) Walsh, M. R.; Koh, C. A.; Sloan, D. E.; Sum, A. K.; Wu, D. T. *Science* **2009**, *326*, 1095−1098.

(20) Tung, Y. T.; Chen, L. J.; Chen, Y. P.; Lin, S. T. *J. Phys. Chem. B* **2010**, *114*, 10804−10813.

(21) Alavi, S.; Ripmeester, J. A.; Klug, D. D. *J. Chem. Phys.* **2007**, *126*, 124708.

(22) Miyoshi, T.; Ohmura, R.; Yasuoka, K. *J. Phys. Chem. C* **2007**, *111*, 3799−3802.

(23) English, N. J.; Macelroy, J. M. D. *J. Comput. Chem.* **2003**, *24*, 1569−1581.

(24) Landín-Sandoval, J. V.; Castillo-Borja, F.; Bravo-Sánchez, I. U.; Vázquez-Román, R. *Comput.-Aided Chem. Eng.* **2009**, *26*, 87−92.

(25) Myshakin, E. M.; Jiang, H.; Warzinski, R. P.; Jordan, K. D. *J. Phys. Chem. A* **2009**, *113*, 1913−1921.

(26) English, N. J.; Phelan, G. M. *J. Chem. Phys.* **2009**, *131*, 074704.

(27) Alavi, S.; Ripmeester, J. A. *J. Chem. Phys.* **2010**, *132*, 144703.
(28) Iwai, Y.; Nakamura, H.; Arai, Y.; Shimoyama, Y. *Mol. Simul.* **2010**, *36*, 246−253.
(29) English, N. J.; Tse, J. S. *Phys. Rev. Lett.* **2009**, *103*, 015901.
(30) English, N. J.; Tse, J. S.; Carey, D. J. *Phys. Rev. B* **2009**, *80*, 134306.
(31) Anderson, B. J.; Tester, J. W.; Borghi, G. P.; Trout, B. L. *J. Am. Chem. Soc.* **2005**, *127*, 17852−17862.
(32) Gomez-Gualdrón, D. A.; Balbuena, P. B. *J. Phys. Chem. C* **2007**, *111*, 15554−15564.
(33) Kuznetsova, T.; Sapronova, A.; Kvamme, B.; Johannsen, K.; Haug, J. *Macromol. Symp.* **2010**, *287*, 168−176.
(34) Hawtin, R. W.; Quigley, D.; Rodger, P. M. *Phys. Chem. Chem. Phys.* **2008**, *10*, 4853−4864.
(35) Jacobson, L. C.; Hujo, W.; Molinero, V. *J. Phys. Chem. B* **2010**, *114*, 13796−13807.
(36) Ripmeester, J. A.; Alavi, S. *ChemPhysChem* **2010**, *11*, 978−980.
(37) Soullard, J.; Santamaria, R.; Cruz, S. *Chem. Phys. Lett.* **2004**, *391*, 187−190.
(38) Santamaria, R.; Soullard, J. *Chem. Phys. Lett.* **2005**, *414*, 483−488.
(39) Soullard, J.; Santamaria, R.; Jellinek, J. *J. Chem. Phys.* **2008**, *128*, 064316.
(40) Santamaria, R.; Soullard, J.; Jellinek, J. *J. Chem. Phys.* **2010**, *132*, 124505.
(41) Hill, T. L. *Nano Lett.* **2001**, *1*, 273−275.
(42) U.S. Department of Energy. http://www.fossil.energy.gov/programs/oilgas/hydrates (accessed Sep 1, 2011).
(43) McMullan, R. K.; Jeffrey, G. A. *J. Chem. Phys.* **1965**, *42*, 2725−2732.
(44) Soullard, J.; Santamaria, R.; Boyer, D. *J. Phys. Chem. A* **2011**, *115*, 9790−9800.
(45) Ghosh, D. C.; Biswas, R. *Int. J. Mol. Sci.* **2002**, *3*, 87−113.
(46) Becke, A. D. *J. Chem. Phys.* **1988**, *88*, 2547−2553.
(47) Becke, A. D. *Phys. Rev. A* **1988**, *38*, 3098−3100.
(48) Lee, C.; Yang, W.; Parr, R. G. *Phys. Rev. B* **1988**, *37*, 785−789.
(49) Kaestner, J. *DL-FIND Geometry optimization subroutine*; STFC Daresbury Laboratory, Revision 406, 2006.
(50) Friedrichs, M. S.; Eastman, P.; Vaidyanathan, V.; Houston, M.; Legrand, S.; Beberg, A. L.; Ensign, D. L.; Bruns, C. M.; Pande, V. S. *J. Comput. Chem.* **2009**, *30*, 864−872.
(51) Ufimtsev, I. S.; Martinez, T. J. *J. Chem. Theory Comput.* **2009**, *5*, 2619−2628.
(52) Kästner, J.; Carr, J. M.; Keal, T. W.; Thiel, W.; Wander, A.; Sherwood, P. *J. Phys. Chem. A* **2009**, *113*, 11856−11865.
(53) Vinet, P.; Rose, J. H.; Ferrante, J.; Smith, J. R. *J. Phys.: Condens. Matter* **1989**, *1*, 1941−1963.
(54) Li, J. H.; Liang, S. H.; Guo, H. B.; Liu, B. X. *Appl. Phys. Lett.* **2005**, *87*, 194111.
(55) Rose, J. H.; Smith, J. R.; Guinea, F.; Ferrante, J. *Phys. Rev. B* **1984**, *29*, 2963−2969.
(56) Chen, L. R.; Chen, Q. H. *J. Phys.: Condens. Matter* **1989**, *3*, 775−780.
(57) Kumari, M.; Dass, N. *J. Phys.: Condens. Matter* **1990**, *2*, 7891.
(58) Fei, Y.; Mao, H. K.; Hemley, R. J. *J. Chem. Phys.* **1993**, *99*, 5369−5373.
(59) Dieter, G. E. *Mechanical metallurgy*; McGraw-Hill: London, 1976; Chapt. 2, sect. 11.
(60) The densities of clathrate methane in the *sI* and *sII* conformations were taken from example 5.2 of the Sloan's book.[1] The expressions used there were obtained after a statistical thermodynamic approach to hydrate phase equilibria.